Volume phase holographic gratings: large size and high diffraction efficiency

Pierre-Alexandre Blanche
Patrick Gailly
Serge Habraken, MEMBER SPIE
Philippe Lemaire
Claude Jamar, MEMBER SPIE
Centre Spatial de Liège
Av. du Pré-Aily
B-4031 Angleur, Belgium
E-mail: plemaire@ulg.ac.be

Abstract. Volume phase holographic gratings (VPHGs) possess unique properties that make them attractive for numerous applications. After reviewing major VPHG characteristics through theory, we discuss some aspects of the dichromated gelatin recording material and the holographic recording process. The large-scale VPHG research facility set up at the Center Spatial de Liège enables production of VPHGs up to 380 mm in diameter, with fringe frequencies from 315 to 3300 lp/mm. We describe the work that has been undertaken in our laboratory to remove the last limitations inherent in VPHGs. [DOI: 10.1117/1.1803557]

Subject terms: dichromated gelatin; spectrograph; grating; holography; heads-up display.

Paper 0431124 received Dec. 9, 2003; revised manuscript received May 21, 2004; accepted for publication Jul. 19, 2004. This paper is a revision of a paper presented at the SPIE conference on Specialized Optical Developments in Astronomy, Aug. 2002, Waikoloa, Hawaii. The paper presented there appears in SPIE Proceedings Vol. 4842.

1 Introduction

Volume phase holographic gratings (VPHGs) recently returned to the scientific forefront due to astronomers and the telecom market.[1–3] The requirements for higher diffraction efficiency for spectrometers and demultiplexers revived the dichromated gelatin (DCG) technology, which is nearly 40 yr old.[4] Indeed, this kind of grating has demonstrated capabilities for 70 to 99% efficiency from near UV to IR. But new applications require new developments to achieve the modern goals in term of size, bandwidth, wavefront, thermal behavior, etc.

From the heritage of several diffractive and holographic projects and applications, the Center Spatial de Liège (CSL) has developed a large-scale DCG VPHG facility. This paper first reviews the major VPHG properties and the advantages of the DCG recording material. Then, we briefly present the new CSL facility, to focus on the research projects and breakthroughs.

We describe the high-line frequency regime of VPHGs, the reasons why large-index modulation is so important, and the gelatin grating behavior in a cryogenic environment. We present a mosaic solution for even larger gratings and a postpolishing technique to correct the diffracted wavefront. The field of holographic mirrors for head-up displays is also tackled.

2 VPHGS and DCG Properties

Rather than being diffracted by surface-relief structures, as with a usual grooved grating, the light going through a VPHG undergoes diffraction due to bulk refractive index modulation. The transmission VPHG geometry that is used throughout this paper is defined in Fig. 1. The grating parameters are incidence angle α, diffraction angle β, slant angle γ, grating vector $\mathbf{K}$, grating thickness d, grating period Λ, the frequency of the intersection of the grating fringes with the grating surface ν, and mean index of refraction n. Subscript number indicate the considered medium.

Light is diffracted at angles according to the classical grating equation:

$$m\nu\lambda = \sin\alpha_0 + \sin\beta_0, \tag{1}$$

where m is an integer giving the order of diffraction, and λ the wavelength of light in free space.

The Bragg equation, for a plane transmission VPHG with unslanted fringes ($\gamma=\pi/2$ and thus $\Lambda=1/\nu$), is given by

$$m\lambda = \Lambda 2 n_1 \sin\alpha_1, \tag{2}$$

where

$$n_1 \sin\alpha_1 = n_0 \sin\alpha_0, \tag{3}$$

where n_0 is assumed to be unity for air.

The Bragg condition is met when the wavelength and fringe spacing are such that the angle of incidence and diffraction are equal and opposite.

The diffraction mechanism of a VPHG occurs through the bulk material and without absorption modulation. That gives rise to unique properties particularly useful for many applications:

1. Theoretical efficiency of 100% can be achieved.
2. Transmission or reflection gratings can be produced. This depends only on the Bragg planes orientation.
3. The undiffracted wavelengths going through the grating are not perturbed and can be reused for further purposes.

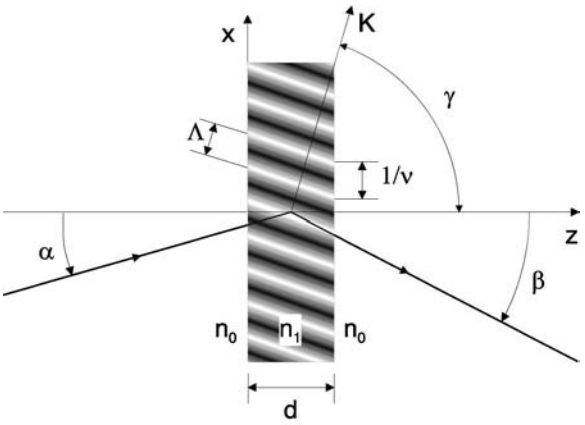

Fig. 1 Transmission VPHG geometry and parameters. Index modulation is represented by the gray pattern.

4. The blaze curve depends of the incidence angle. That generates the ''superblaze.''

Since superblaze is an unusual but extremely attractive property of VPHGs, it is important to spend some time explaining it. The so-called blaze curve is the diffraction efficiency measured according to the wavelength. It depends on the light incidence angle and achieves its maximum at the Bragg angle. The envelope of the blaze curves measured at various incidence angle is called the superblaze. An example of this significant behavior is presented in Fig. 2. Superblaze property is used to enlarge the VPHG frequency domain since diffraction at different wavelengths is optimized simply by rotating the grating.

Major properties of the VPHGs can be straightly deduced from the Bragg law and the Kogelnik's two-wave coupled-wave theory.[5] This theory is the most popular base for computation of thick volume gratings and is extremely accurate even though the index modulation is sinusoidal and the thick grating criteria are respected[6]:

$$n_1(x,z) = n_1 + \Delta n_1 \cos[(2\pi/\Lambda)(x \sin\gamma + z\cos\gamma)], \tag{4}$$

$$\rho \equiv 2\lambda^2/\Lambda^2 \Delta n_1 \geqslant 10, \tag{5}$$

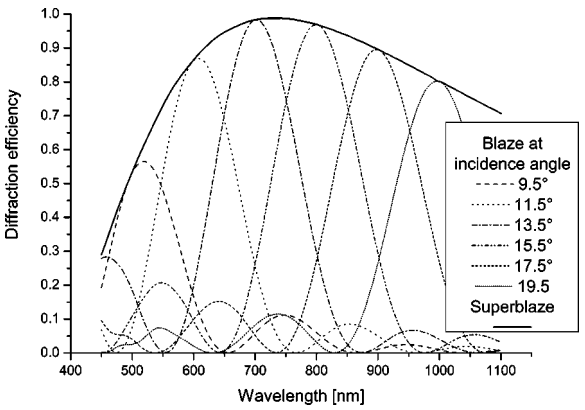

Fig. 2 Simulated blaze curves at various incidence angles and the consequent superblaze for a VPHG with the following characteristics: $\Delta n = 0.024$, $d = 15\ \mu$m, $\Lambda = 1000$ lp/mm, and $\lambda_B = 735$ nm.

$$Q' \equiv 2\pi\lambda d/n_1\Lambda^2 \cos\alpha_1 > 1, \tag{6}$$

and

$$d/\Lambda > 10. \tag{7}$$

The most significant results of the two-wave coupled-wave theory for our purpose is that the diffraction efficiency η, spectral bandwidth $\Delta\lambda$, and angular bandwidth $\Delta\alpha$ are functions of the intensity of the grating modulation Δn_1 and thickness. For a plane transmission grating with unslanted fringes, the TE mode (polarization perpendicular to the incidence plane) diffraction efficiency at the first Bragg order is given by

$$\eta_{\mathrm{TE}} = \sin^2[\pi\Delta n_1 d/(\lambda\cos\alpha_1)]. \tag{8}$$

The first-order spectral bandwidth and angular bandwidth are approximated by

$$\Delta\lambda_{\mathrm{FWHM}}/\lambda \approx (\Lambda/d)\cot\alpha_1, \tag{9}$$

$$\Delta\alpha_{\mathrm{FWHM}} \approx \Lambda/d, \tag{10}$$

where $\Delta\alpha_{\mathrm{FWHM}}$ is expressed in radians.

One can see directly through these relations that the challenge, when producing VPHGs, is to induce the right index modulation into the precise thickness to achieve the proper efficiency and bandwidth.

The polarization dependency on the VPHGs occurs through the reduced effective coupling constant $\cos(2\alpha_1)$. For the TM mode (polarization parallel to the plane of incidence), the diffraction efficiency equation becomes

$$\eta_{\mathrm{TM}} = \sin^2[\pi\Delta n_1 d\cos(2\alpha_1)/(\lambda\cos\alpha_1)], \tag{11}$$

As long as α_1, the incidence angle within the medium, is small, polarization dependencies are minimized.

When grating parameters do not match the thick grating criteria, or the index modulation is not sinusoidal, the more accurate rigorous coupled-wave analysis (RCWA) from Gaylord and Moharam[7,8] is required to calculate the hologram diffraction properties. Since 1994, CSL has developed its own RCWA code. This powerful tool is very flexible to study specific gratings dealing with small-layer, high-grating-period or high-index modulation such as those presented in the next sections.

In addition of being privileged by theory, VPHGs can be recorded into an exceptional material: DCG. Used for nearly 40 years for volume phase holograms[4] (VPH), DCG is recognized worldwide as an outstanding recording material.[9] Indeed, its properties are

1. DCG can hold the uppermost refractive index modulation ($\Delta n > 0.1$) (see Sec. 4.2).
2. Its absorption is negligible from the near UV to the IR as far as 2.7 μm, which enables its use over a very large spectral range.[1]
3. When it is properly processed, there is no scattering.

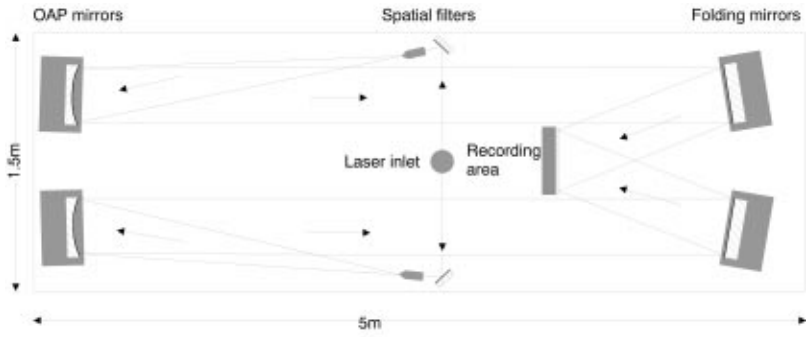

(a) Set-up geometry. Fringe frequency 1500 lp/mm.

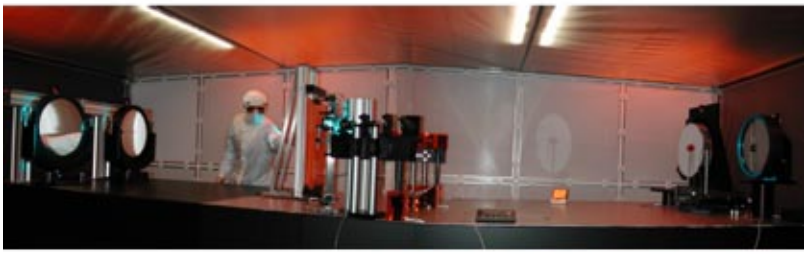

(b) Laboratory picture.

Fig. 3 Holographic recording setup.

4. Its spatial resolution is dimensionally molecular. DCG can store from a few hundred to several thousand lines per millimeter (see Sec. 4.1)
5. Once gelatin is processed and properly sealed, the properties of the recorded grating are stable over tens of years and it has a excellent resistance to temperature changes (see Sec. 4.3).
6. The recording process is holographic and its sensitivity is within the reach of common lasers such as argon ions.
7. Its mean refractive index is close to 1.5, so a common glass coating induces no interface reflection.
8. The raw materials are inexpensive and can be purchased in large quantities.

The only DCG drawbacks are that it is hygroscopic and it suffers from rapid aging when stored unprocessed. This requires the preparation of the DCG a few days before being recorded and, once processed, the grating must be protected from humidity. These are the main reasons why attempts to commercialize DCG were unfruitful.

The DCG recording technique is a well-known holographic method. Two coherent beams cross each other inside the sensitive medium, interfering and inducing a succession of chemical changes.[10] This technique brings the following inherent advantages:

1. It can likely produce a very large grating size (several hundred of centimeters square).
2. Complex grating structures can easily be made, diffracting a wavefront according to defined shape. These holograms are called holographic optical elements (HOEs).
3. It avoids the defects encountered with ruled structures such as ghosts.
4. Grating customization is relatively straightforward and each grating is an original rather than a replica.

After recording, the DCG processing is basically constituted of three steps. First, the dichromate is removed by a photographic fixer. Second, the gelatin is soaked in baths with increasing concentration of isopropyl alcohol, starting with pure water and ending with pure alcohol. Finally, the solvent is removed by heating the gelatin. There are many papers concerning the best way to process gelatin according to the desired application.[10–14]

3 CSL Facilities and Setup

Producing a VPHG with DCG requires three steps: coating the gelatin, recording the hologram, and processing the gelatin to obtain a stable final product. The CSL facilities have been scaled to accommodate blanks up to 40×40 cm. The DCG coating machine can hold 50×70×3 cm flat glass. Optical quality is obtained on 40×60-cm gelatin layers from 5 to 25 μm and when dried it can be coated with 20% peak-to-valley deviation over the full surface.

Recording is performed on a 1.5×5-m optical bench. The laser source is an argon laser Innova Sabre™ TSM 25 from Coherent, which can deliver 4.8 W at 488 nm. The setup geometry and a picture of the recording laboratory are shown in Fig. 3. The argon laser beam comes up from a hole drilled into the center of the table. It is split into two beams having the same intensity and polarization (not mandatory). They are then filtered with pinholes standing high energy. To ensure homogeneous illumination in the sample area, beams are broadened to nearly twice the useful diam-

eter. Two off-axis parabolic mirrors collimate the useful beams. Their clear aperture diameter is 395 mm with a focal length of 200 cm. To adjust illumination angle, two flat mirrors with a 400-mm clear aperture diameter fold the beams. Following the Bragg law [see Eq. (2)], the recorded fringe frequency $1/\Lambda$ can be changed continuously from 315 to 3300 lp/mm. Higher frequencies can, of course, be recorded in DCG layer. For this case, the recording setup should include large-scale prisms to increase the beam angles within the recording medium.

Due to edge diffraction, the desired optical quality for the recording beams is achieved on a diameter up to 380 mm.

Note that this setup is not proprietary to DCG but can be used for holographic recording onto other media such as photopolymers, photoresine, silver halogenure emulsions, etc. In a same way, the setup can be used to record holographic mirrors or HOEs.

The development laboratory is set up with thermostated baths. Inner baths are 53×65 cm. Forced convection oven with interior dimensions of $80\times60\times50$ cm dries the developed holograms.

These three laboratories, i.e., for coating, exposure, and development, are air conditioned in both temperature and hygrometry, since fresh gelatin is sensitive to these parameters. Following the technical heritage of CSL in space optical payload qualification, laminar fluxes maintain laboratories as class 100 clean rooms.

Our goal is to control each process step to produce very high quality holograms. Therefore, metrology and certification play an important part of our effort.

Dry gelatin thickness is measured with a fiber spectrometer according to parallel and perpendicular coating axis. This technique enables a 1-mm spatial resolution and a 0.1-μm thickness. Using this apparatus, we make sure there is no unwanted wave or tilt in the gelatin layer and we certify specifications before recording the hologram.

Recording setup geometry is tuned by theodolite measurement and autocollimation. The OAP position is checked by large (85-mm-aperture) shear plates and interferometry. During recording, phase compensation is activated by a piezoelectric transducer, locking the fringe position at the recording location.

Diffraction efficiency and diffracted phase are monitored over the full hologram surface using an interferometer. The latter is installed directly after one of the spatial filters of the recording setup to take advantage of the large optics. The diffracted beam is retroreflected by a flat mirror placed behind the hologram. To correct the phase from distortion introduced by the whole system, we subtract the phase recorded without any sample.

The diffraction efficiency map is measured by blocking the reference beam of the interferometer. Thus, we record an image diffracted back and forth by the hologram.

We use optical fiber spectrometers to measure blaze and superblaze curves into the wavelength ranges of 450 to 1100 and 1100 to 2500 nm. A most representative hologram position is chosen according to the information coming from the diffraction efficiency map. To avoid problems due to light collection into the fiber of the spectrometer, we usually do not measure the diffraction efficiency (first order). Instead, we measure the transmitted light (zero order). Transmission and diffraction intensity are simply related by the following equation:

$$I_{\text{transmitted}} = I_{\text{incident}} - I_{\text{diffracted}} - I_{\text{lost}},$$

where I_{lost} stands for light lost, i.e., reflection at material interfaces, absorption, or scattering.

Using our own RCWA code, the experimental blaze and superblaze data are interpolated to determine the grating characteristics. The hologram index modulation Δn_1 is accessible by this way, as we see in the next section.

4 Special Gratings and Developments

VPHGs of various size, blaze wavelength, spatial frequency, etc. have already been produced by the CSL. Several astronomic spectrometers are currently running with those gratings in different configurations: Littrow, fixed diffraction configuration, or variable incidence for superblaze. In this section, we describe the most representative gratings or, at least, the most challenging, and we discuss the developments carried out in our labs.

4.1 *High-Line Frequency*

For many applications, the most important parameter after the diffraction efficiency is the dispersion of the grating. The angular dispersion is straightly deduced from the classical grating Eq. (1) by holding α_0 constant and differentiating with respect to β_0:

$$\mathrm{d}\beta_0/\mathrm{d}\lambda = m\nu/\cos\beta_0, \tag{12}$$

or, for an unslanted grating ($\Lambda = 1/\nu$):

$$\mathrm{d}\beta_0/\mathrm{d}\lambda = m/\Lambda\cos\beta_0. \tag{13}$$

It is very attractive to increase the number of lines per millimeter when using the grating as a dispersive element. But the grating efficiency should not be traded off.

Actually, the coupling constant between TE and TM mode is $\cos(2\alpha_1)$ [see Eqs. (8) and (11)] and, according to the Bragg law [Eq. (2)], α_1 increases when Λ decreases. Thus, a higher number of lines per millimeter means larger difference between TE and TM efficiency.

For line frequencies ranging from 300 to 2000 lp/mm, TE and TM diffraction modes can be maximized for the same wavelength. Unfortunately, for higher line frequencies, diffraction according to TE and TM modes is maximum for different wavelengths and, thus, unpolarized light can not be fully diffracted. This phenomenon is simulated by rigorous coupled wave calculation in Fig. 4(a), where the index modulation was chosen such that TE is at its first maximum [see Fig. 4(b)]. For unpolarized light, the efficiency reaches only 63% for the 525-nm central wavelength. Still, by tuning the index modulation to three times what is required to use the first diffraction TE peak, the second TE maximum matches the first TM maximum, as shown in Fig. 4(b). For these parameters, it is possible to obtain a theoretical 100% diffraction efficiency for unpolarized light at the blaze wavelength.

The challenge for this kind of grating is to reach such a high index modulation without making the gelatin milky. CSL successfully produced two 170×120-mm, 3300 lp/mm

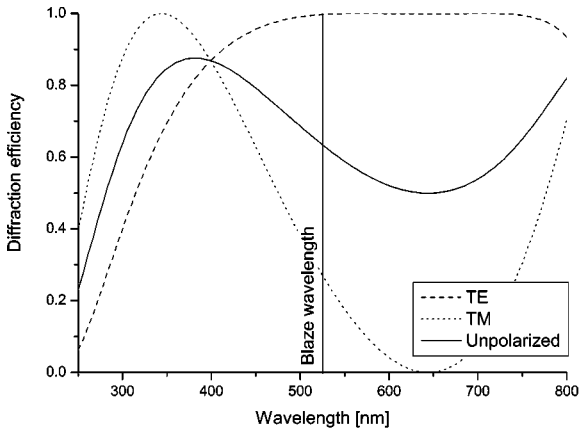

(a) Superblaze. $\Delta n = 0.021$

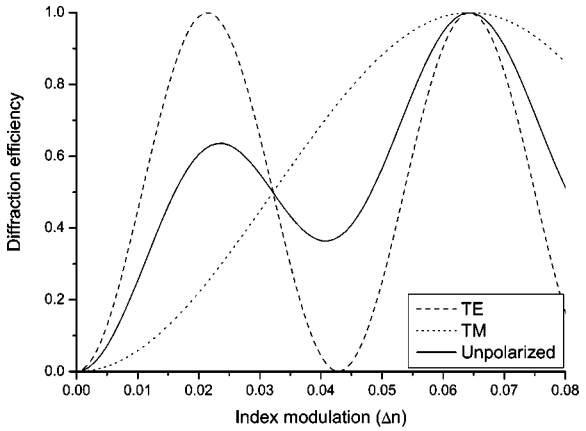

(b) Efficiency at the Blaze wavelength according to index modulation

Fig. 4 RCW diffraction efficiency calculation of a high-line-frequency VPHG. Parameters are $1/\Lambda = 3300$ lp/mm, $d = 10\ \mu$m, $\lambda_{Blaze} = 525$ nm.

gratings with $\Delta n = 0.048$ (according to RCW fitting) without any visual scattering. An example of transmission spectrum is shown in Fig. 5, where RCW interpolation of both blaze and superblaze is superimposed. Fitting parameters are $\Delta n = 0.048$, $d = 12\ \mu$m, and $1/\Lambda = 3300$ lp/mm.

4.2 *High-Index Modulation*

Having a highly dispersive grating is fine, but increasing the line density has an impact on the bandwidth [see Eqs. (9) and (10)]. To maintain an acceptable bandwidth while reducing Λ, one must also reduce d, the grating thickness.

In other respect, the coupled-wave equations for efficiency also include the grating thickness [see Eqs. (8) and (11)]. To keep the efficiency to its highest value when the grating thickness is reduced, the index modulation needs to be increased.

The gelatine index modulation is linked to its processing, and we improved our method by a better thermal control of the development bathes and so reached the highest index ever. We obtained an 80×80-mm VPHG with

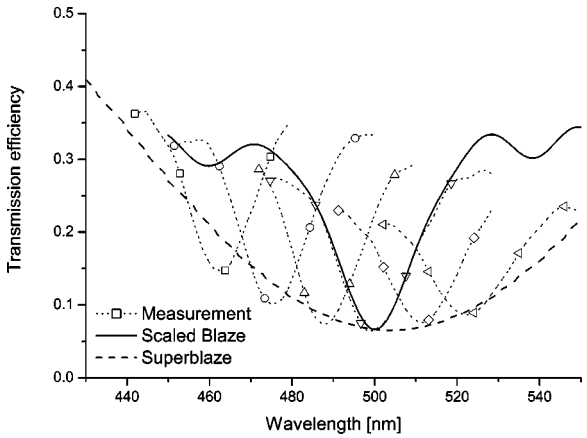

Fig. 5 Transmission efficiency of a 3300 lp/mm VPHG with blaze and superblaze RCW interpolation.

2.9-μm gelatin thickness and a modulation of 0.14, as calculated by RCWA. Scattering, often present in highly modulated gelatin, is not visible with naked eye in our sample. Figure 6 shows the zero-order transmission efficiency according to the wavelength at the Bragg angle of 45 deg. Measurements are interpolated by RCWA calculation and scaled to take losses (mostly reflection) into account.

Achieving very high index modulation is also extremely important to diffract IR wavelengths. Once again, looking at the coupled-wave equations of diffraction [Eqs. (8) and (11)], if wavelength increases, the modulation must also increase to keep the diffraction close to unity. This could also be intuitively understood by optical pathway difference: the larger the wavelength, the larger the optical pathway difference must be to obtain a constructive interference.

The subject of VPHGs for the IR raises another problem: the cryogenic behavior of the material.

4.3 *Cryogenic Behavior*

The astronomical IR domain of observation is currently surfing on the top of the wave. Potential for organic mol-

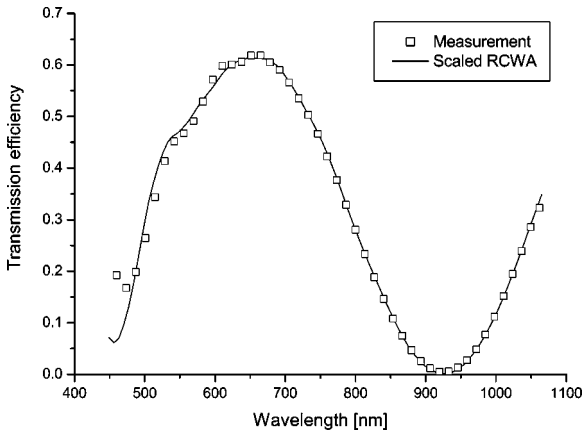

Fig. 6 TE transmission efficiency measurement and RCWA interpolation at the Bragg angle. Calculation parameters are $d = 2.9\ \mu$m, $\Delta n = 0.14$, $1/\Lambda = 1555$ lp/mm, and $\alpha_0 = 45$ deg.

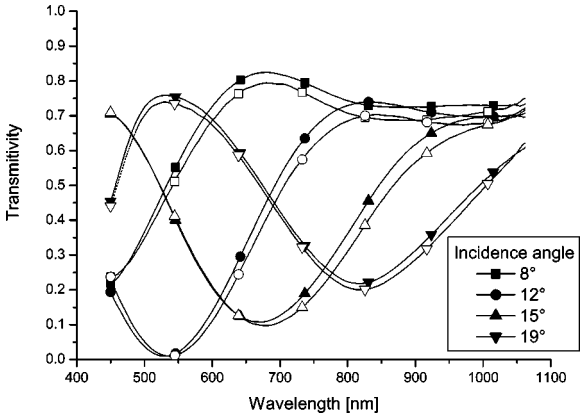

Fig. 7 Comparison of the transmission spectra recorded at 22°C (solid symbols) and at −180°C (hollow symbols) for various incidence angles.

ecules detection is one of the reasons why this wavelengths region is so attractive. Not to be blinded by instrument radiations, IR spectrometers must operate at cryogenic temperature (around 100 K). To propose VPHGs as IR dispersive element, CSL developed and tested gratings that stand and perform at low temperatures.

''Low temperature'' samples were made by changing slightly the development process, raising the oven temperature to ensure a complete solvent evaporation. The gelatin layer was sandwiched between 3-mm-thick and 8×8-cm glass plates. The stack is fitted together with optical glue. To fit into the measurement range of our spectrometer, the blaze wavelength was not set in the IR but in the visible. But, this does not at all influence the cryogenic certification.

The cryogenic measurement setup is constituted of a vacuum vessel with two wide glass windows and a liquid nitrogen coil, which cool down the sample mount. The sample is inserted between two copper plates that ensure thermal conductivity. Four thermocouples are fixed in different locations to measure the sample temperature. A fiber spectrometer records the sample zero-order spectrum through the vessel windows. A rotating stage enables us to change the incidence angle to measure the superblaze. The probe beam size is around 1 cm in diameter.

To make sure the grating could physically stand cold temperatures, we took pictures of the grating before cooling it. After 1 h at −180°C (93 K), absolutely no visible defect was observed on the sample (i.e., no cracks, scattering, spots, milkiness, etc.).

Afterward, we have measured the blaze of a new sample at various temperatures: ambient (22°C), −50, −100, −150, and −180°C. Then, we let the sample remain for 6 h at −180°C and warmed it before measuring the blaze once again at ambient temperature.

Measurements displayed in Fig. 7 show blaze curves recorded at various incidence angles before cooling and at −180°C. An undirectional deviation of less than 5% is to notice. This stands within the measurement uncertainty: rotating stage repositioning within 0.5 deg, thermal dilatation of the sample mount, source spectrum change, etc. Thus, the efficiency does not significantly decrease during or after the grating cooling and, even more important, blaze and superblaze curves do not change.

It remains to conduct thermal cycling experiment to ensure there is no long-term damage. Blank quality could also be an issue if the thermal dilatation coefficient is very different from the gelatin or the glue. Finally, we must test the wavefront distortion when the grating is subjected to cryogenic temperature.

4.4 *Large-Size Monolithic VPHG*

The initial purpose of our facility was the production of large-size monolithic VPHGs for astronomical spectrometers. By 2000, and according to astronomer's prospects, the gratings size must be at least 300 mm of diameter. However, the larger the optics of the recording setup, the higher their price and the harder it is to stabilize them at an acceptable level for interferometry. Moreover of the mirrors direct cost, larger optics require more laser power to illuminate the whole hologram surface. All things considered, we purchased two 395-mm clear aperture out-of-axis parabolic mirrors (OAPs) to collimate beams from a 25-W Coherent Innova Sabre laser.

The largest monolithic VPHGs we have produced up to now are two 380-mm-diam gratings for gOlem: Osservatorio Astronomico di Brera (Italy). Their specifications were

1. Brera blue line frequency≈1200 lp/mm, central wavelength=475 mn
2. Brera red line frequency≈500 lp/mm, central wavelength=850 mn

Blanks were float glass squares with 400 mm sides. A picture of one of those gratings can be seen in Fig. 8, where the light from an halogen lamp is diffracted to a screen.

4.5 *Mosaiced VPHG*

Whatever the size of the facility, it will always be limited and this will restrain the instrument designer creativity. To overcome this problem, we tested the mosaic technique, which consists of assembling several gratings recorded and processed independently.

The challenges are that mosaic subelements must diffract at exactly the same angle and efficiency, which means gelatin layer thickness and index modulation must be perfectly tuned to produce the same blaze and superblaze, element to element. The assembly technique must minimize edge diffraction and shading as providing fine alignment of the gratings ensuring diffraction to the same direction.

Two mosaics have been produced for the National Optical Astronomy Observatory (NOAO), both constituted of four elements. The total size is 240×340 mm. Subelement orientation was ensured during the encapsulation process by monitoring the diffracted pattern of an extended HeNe beam.

A diffraction picture of such a mosaic VPHG is shown in Fig. 9. Note that both diffracted spectra, cast to the screen and coming from the upper and lower subgratings, are strictly parallel and do not diverge or interpenetrate each other. This is one obvious sign that the elements are well aligned.

Using that mosaic technique, the setup size no longer matters and the final grating size can be as large as desired.

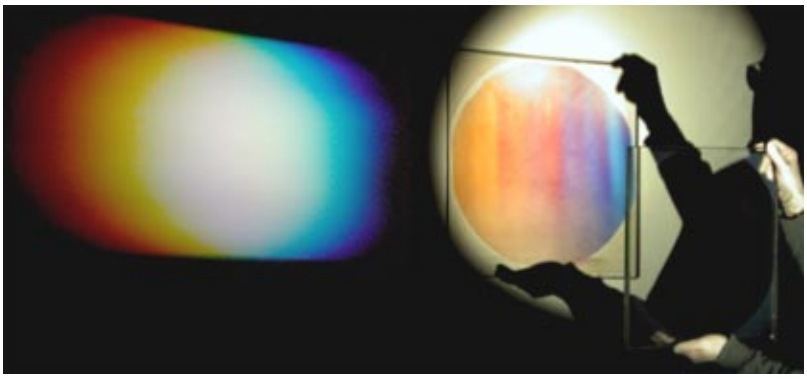

Fig. 8 Picture of a 380-mm-diam grating produced by CSL.

4.6 *Postpolishing*

Wavefront flatness can be mandatory for some applications, especially in new spectrographs that are intended to be diffraction limited instruments, not to mention, the space-based missions. These highly stringent observatories require dispersive elements with distortion less than $\lambda/4$.

Several factors influence the diffracted wavefront from a VPHG element:

1. the gelatin thickness homogeneity
2. the recording setup alignment
3. the blank and cover homogeneity as their outer face flatness
4. the gelatin tension during processing
5. shrinkage of the optical cement used to glue the grating cover

The three first parameters are very well mastered and are no longer major sources of wavefront distortion. However, the gelatin and optical cement shrinkage during their process can not be avoided. Their combination can lead, on large VPHGs, to wavefront errors of several wavelengths. One solution is to postpolish the blanks after the VPHG has been encapsulated.[15]

The VPHG wavefront error can be a complex function without any symmetry. This is rather difficult to correct by conventional polishing. Thus, we chose to use an ion-beam figuring technique where an ion gun projects particles to the blank, which etches the glass. The time that the ion beam remains on a blank location is calculated according to the measured wavefront and ablation profile. Thus, the right amount of material is removed.

Note that a VPHG acts as an hologram (diffractive element) and not like a conventional lens (refractive element). The diffracted beam has a reconstructed wavefront, depending on the recording beams geometry. Changing the light entrance side or the Bragg angle sign will determine which beam is reconstructed and, thus, the amplitude and/or the sign of the diffracted wavefront error will change.

This characteristics are shown in Figs. 10(a) and 10(b), where two Zygo interferometer measurements are reproduced. For both figures, the laser beam coming from a Zygo is diffracted by the VPHG, and then is retroreflected by a mirror ($\lambda/20$) back to the grating, where it is diffracted one more time to reenter the interferometer. From Fig. 10(a) to Fig. 10(b), the entrance side of the laser beam has changed and so has the sign of the wavefront error.

This symmetry specificity must be taken into account for the wavefront correction but also when the VPHG is used. To pinpoint this behavior, we postpolished one outer face of the grating introduced in Fig. 10. Figure 11 shows that the diffraction from one direction is now flattened to $\lambda/6$ [Fig. 11(a)]. But, at the same time, the wavefront diffracted to the other direction deteriorated to 0.7λ root mean square (rms) [Fig. 11(b)].

The postpolishing technique is very effective to correct the VPH diffracted wavefront. However, care must be taken to use the VPHG with the right orientation. Otherwise, rather than benefit from a corrected wavefront, this latter is twice distorted.

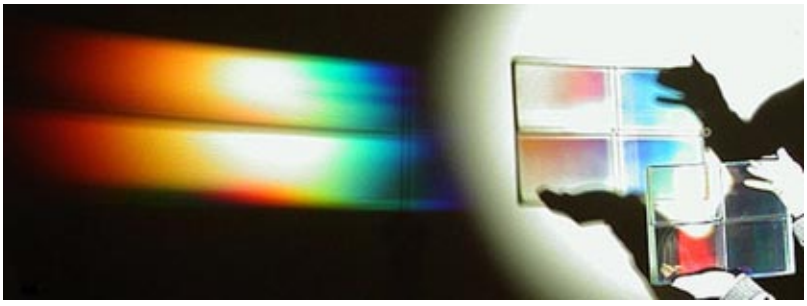

Fig. 9 Picture of a mosaiced VPHG diffracted spectrum.

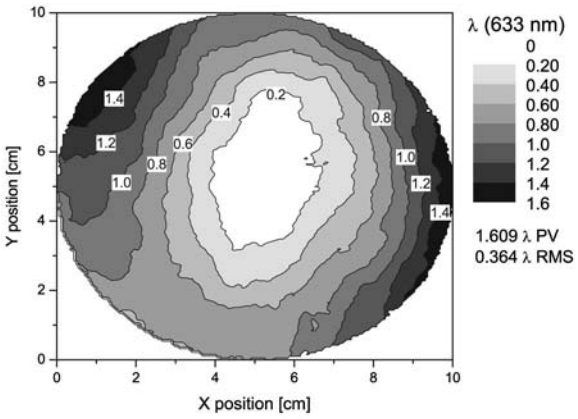

(a) Laser beam entering face A to B

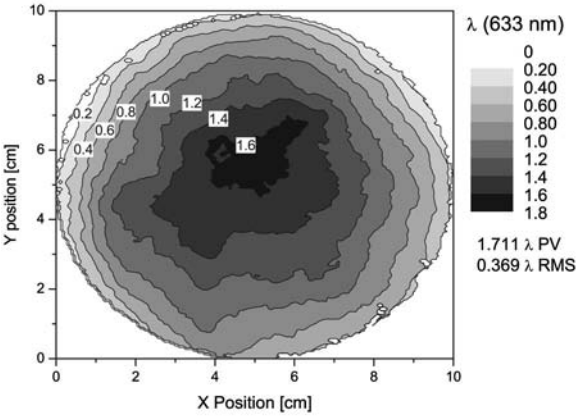

(b) Laser beam entering face B to A

Fig. 10 Diffracted wavefront error according to the grating orientation.

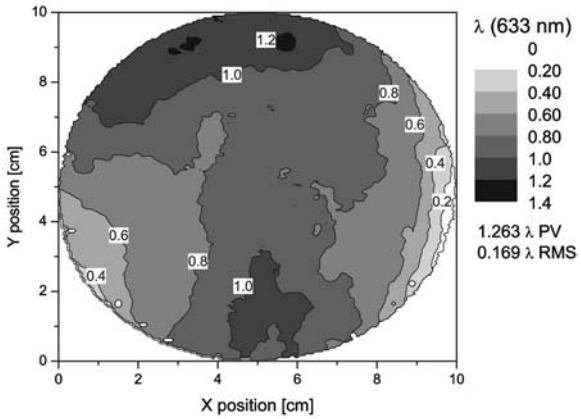

(a) Laser beam entering face A to B

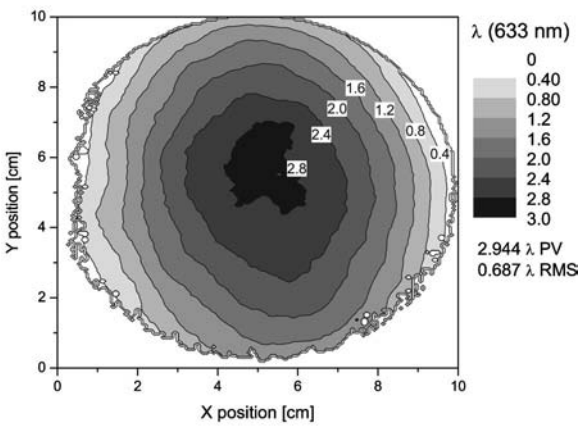

(b) Laser beam entering face B to A

Fig. 11 Diffracted wavefront error according to the grating orientation after beam figuring.

4.7 *Holographic Mirrors*

We presented transmission VPHGs where Bragg planes are oriented more or less perpendicularly to the blank surface and the diffracted beam leaves the grating at the opposite side of the input beam (see Fig. 1). However, by slightly changing the holographic setup, directing laser beams side to side of the gelatin layer, Bragg planes can be recorded approximately parallel to the surface (see Fig. 12). In this case, the diffracted beam comes out by the same side of the grating as the incident beam. As for a dielectric multilayer coating, this kind of VPHG acts as a mirror or filter depending on whether one is considering the diffracted or transmitted beams.

But, unlike multilayer coatings, Bragg planes can be recorded with an arbitrary angle according to the gelatin surface. When $\gamma \neq \pi$, the mirror is said to be ''slanted'' and diffraction occurs at the specific angle β, which is different from the incidence angle α. The slanted holographic mirror does not obey to the Snell-Descartes law ''reflection angle equal incidence angle.'' Nevertheless, the angles of incidence and diffraction are symmetric, within the grating medium, according to the fringes plane:

$$\alpha_1 + 2(\pi - \gamma) = \beta_1 .$$

Figure 13 shows the diffraction behavior of a 180−10 deg slanted mirror. The maximum reflection occurs at 675 nm for an diffraction angle of 20 deg, twice the slant angle.

Reflective VPH grating intensity, bandwidth, and the direction of the reflected light can be tuned by changing the gelatin processing or recording angles (see Fig. 14). Holographic mirrors are so very versatile and possess unique properties compared to metallic or multilayer mirrors. Thus, they are found from rejecting the setup for Raman spectroscopy to vehicle head-up displays.

Moreover, exactly as with transmission VPHGs, it is possible to record an arbitrary optical function into the VPH mirror. Such a mirror diffracts the light according to a defined wavefront shape.[10]

5 Conclusions

We showed that VPHGs have unique properties that make them attractive for numerous applications. Even though VPH and DCG technologies have been known for several decades now, new methods and new user requirements always push further the necessity to investigate and develop.

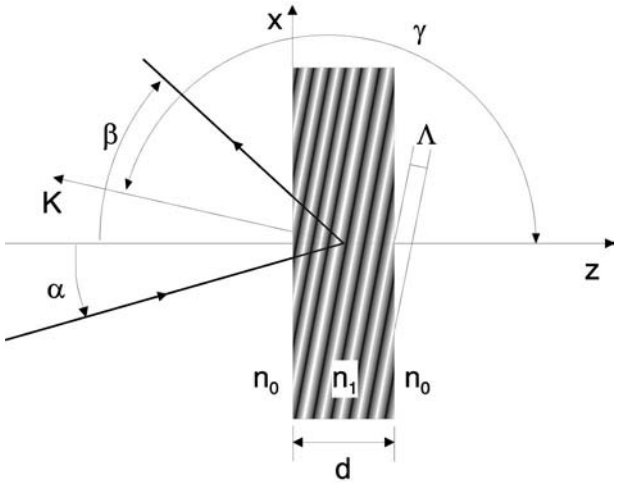

Fig. 12 Reflection VPHG geometry and parameters definition.

CSL fitted out a dedicated facility to produce large-size, high-quality VPHGs and to carry out research projects on this kind of grating. Technics of high-line frequency and high index modulation were tested successfully to enhance the grating dispersion while keeping the advantage of theoretical 100% diffraction efficiency achievable by VPH.

With high index modulation opening the door of the IR regime, we wondered how VPHGs will behave in cryogenic temperature. Our ''low temperature'' gratings have fruitfully stood test down to 93 K, both structurally and operationally.

Holographic recording allows for large size. But, whatever the recording setup size, it will always be limited. Even our facility, which is capable of 380-mm-diam monolithic gratings, is too small for some applications. We tested the mosaic technique, which consists of assembling together VPHGs recorded and processed independently. Using this method, the setup size no longer matters and VPHGs can be as large as desired. Mosaics with 2×2 elements and 340×240-mm total size have been produced.

One other previous limitation of VPHGs was the diffracted wavefront error. The solution we used to correct the wavefront is to postpolish the blank into which the grating

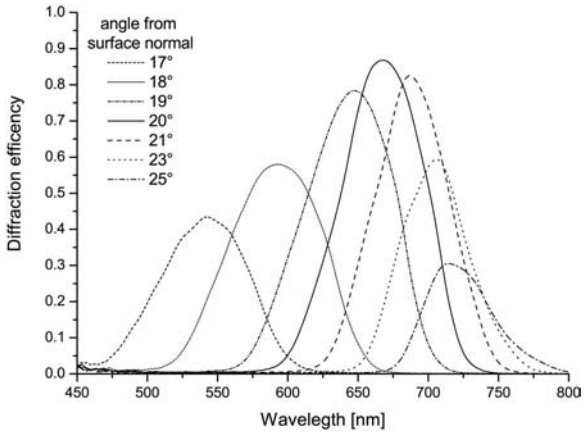

Fig. 13 Reflection efficiency spectrum of a 180 to 10 deg slanted mirror. Incidence light is normal to the surface.

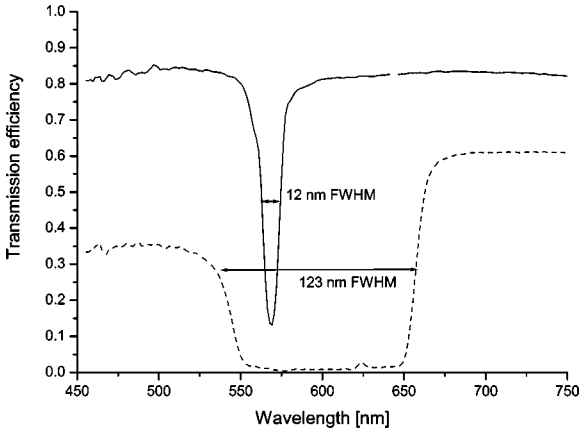

Fig. 14 Transmission efficiency of two mirrors with different bandwidths and central wavelengths.

was encapsulated. The polishing method was ion-beam figuring, which enables complex figures to be worn. Our very first result has demonstrated a capability to obtain λ/6 rms over a 10-cm diameter. Note the fact that wavefront restoration applies only for one specified orientation. Used in the wrong orientation, the grating induces twice the error. This is due to the diffractive nature of the VPH gratings.

We completed this paper with an overview of VPH mirrors. We gave examples of their unique characteristics as fringes slant, which enables us to produce mirrors that no longer obey to the Snell-Descartes law.

Acknowledgments

This work is supported by the Walloon Government under the Contract RW No. 215232. The authors are also acknowledging the EGUNA Astronomer Consortium, directed by the European Southern Observatory for their technical guidance and financial support. Some of the gratings discussed in this paper were manufactured with funding support from the New Initiatives Office of the Association of Universities for Research In Astronomy. The New Initiatives Office is a partnership between two divisions of the Association of Universities for Research in Astronomy (AURA), Inc.: the National Optical Astronomy Observatory (NOAO), and the Gemini Observatory. NOAO is operated by AURA under cooperative agreement with the National Science Foundation (NSF). The Gemini Observatory is operated by AURA under a cooperative agreement with the NSF on behalf of the Gemini partnership: the National Science Foundation (United States), the Particle Physics and Astronomy Research Council (United Kingdom), the National Research Council (Canada), CONICYT (Chile), the Australian Research Council (Australia), CNPq (Brazil), and CONICET (Argentina).

References

1. S. C. Barden, J. A. Arns, and W. S. Colburn, ''Volume-phase holographic gratings and their potential for astronomical applications,'' in *Optical Astronomical Instrumentation*, S. D'Odorico, Ed., *Proc. SPIE* **3355**, 866–876 (1998).
2. G. J. Monnet, H. Dekker, and G. Rupprecht, ''Volume phase holographic gratings at ESO,'' in *Optical Spectroscopic Techniques, Remote Sensing, and Instrumentation for Atmospheric and Space Research IV*, A. M. Larar and M. G. Mlynczak, Eds., *Proc. SPIE* **4485**, 439–444 (2002).

3. J. A. Arns, W. S. Colburn, and S. C. Barden, ''Volume phase gratings for spectroscopy, ultrafast laser compressors, and wavelength division multiplexing,'' in *Current Developments in Optical Design and Optical Engineering VIII*, R. E. Fischer and W. J. Smith, Eds., *Proc. SPIE* **3779**, 313–323 (1999).
4. T. Shankoff, ''Phase holograms in dichromated gelatin,'' *Appl. Opt.* **7**(10), 2101–2105 (1968).
5. H. Kogelnik, ''Coupled-wave theory of thick hologram gratings,'' *Bell Syst. Tech. J.* **48**, 2909 (1969).
6. T. Gaylord and M. Moharam, ''Thin and thick gratings: terminology clarification,'' *Appl. Opt.* **20**(19), 3271–3273 (1981).
7. T. Gaylord and M. Moharam, ''Rigorous coupled-wave analysis of planar-grating diffraction,'' *J. Opt. Soc. Am.* **71**(7), 811–818 (1981).
8. M. G. Moharam and T. K. Gaylord, ''Three-dimensional vector coupled-wave analysis of planar-grating diffraction,'' *J. Opt. Soc. Am.* **73**(9), 1105–1112 (1983).
9. D. Meyerhofer, ''Dichromated gelatin,'' in *Holographic Recording Materials*, H. Smith, Ed., Vol. 20, pp. 75–99, Springer Verlag, Berlin/Heidelberg/New York (1977).
10. J. R. Magarios and D. J. Coleman, ''Holographic mirrors,'' *Opt. Eng.* **24**(5), 769–780 (1985).
11. B. Chang and C. D. Leonard, ''Dichromated gelatin for the fabrication of holographic optical elements,'' *Appl. Opt.* **18**(14), 2407–2417 (1979).
12. S. McGrew, ''Color control in dichromated gelatin reflection holograms,'' *Proc. SPIE* **215**, 24–31 (1985).
13. S. Sjölinder, ''Swelling of dichromated gelatin film,'' *Photograph. Sci. Eng.* **28**(5), 180–184 (1984).
14. O. Salminen and T. Keinonen, ''A comparison of the reflection properties of dichromated gelatin gratings developed in different ways,'' *J. Mod. Opt.* **36**(10), 1377–1383 (1989).
15. S. C. Barden, A. Camacho, and H. Yarborough, ''Post-polishing VPH gratings for improved wavefront performance,'' in *Specialized Optical Developments in Astronomy; Eli Atad-Ettedgui*, S. D'Odorico, Ed., *Proc. SPIE* **4842**, 39–42 (2002).

Pierre-Alexandre Blanche is responsible of the volume phase holographic gratings project held at the Center Spatial de Liège. He received his graduate degree in physics from the University of Liège, Belgium, in 1994. He joined the Center Spatial de Liège and did his PhD on the study of the molecular photo-orientation of azo dyes in polymer matrices for holographic recording. In 2000, he held a post-doctoral position at the University of Arizona, Optical Sciences Center, where he worked on photorefractivity in polymers by two-photon absorption and femtosecond spectroscopy. From 2001 to date, he served as a specialist at the Center Spatial de Liège. His main research interests are science holography, holographic static or dynamic recording materials, non-linear optics and HOE in optical systems.

Patrick Gailly received a BS in physics from University of Louvain-La-Neuve in 1995 and a MS in physics: Optoelectronics in 1996 from University of Liège Belgium. Since joining Center Spatial de Liège in 1996, he has mainly worked in ion beam figuring and related technology. He has performed extensive work in technique development and the study of roughness evolution under ion milling. He is the responsible for ion beam figuring activities at Liège and is also involved in microfabrication projects.

Serge Habraken currently manages the Advanced Optics Research Group at the Center Spatial de Liège. He received his MS in physics and PhD degrees from the University of Liège in 1990 and 1995. For the last 9 years, space optics has been his main research activity, but the wide synergy between technologies has led to his involvement in a variety of application fields. His research interests are focused on holographic optics, new materials and processes in optics, and solar energy applications.

Philippe Lemaire: Biography and photograph not available.

Claude Jamar is currently professor at the University of Liege and Director General of the Liege Space Center. He holds a PhD in astrophysics, and has developed many space instruments for astrophysical and geophysical observations.